Glasses in the System Phosphorus–Sulfur: A ^{31}P Spin-Echo and High-Speed MAS-NMR Study of Atomic Distribution and Local Order

Michael Tullius, David Lathrop, and Hellmut Eckert*

Department of Chemistry, University of California, Santa Barbara, Goleta, California 93106
(Received: May 23, 1989; In Final Form: September 4, 1989)

The structural organization of glasses in the system P–S is investigated by modern solid-state NMR techniques. Throughout the entire region of glass formation, S=$PS_{3/2}$ groups are found to be the principal short-range-order environment. These units are identified, in conjunction with parallel studies of crystalline model compounds, by a characteristic ^{31}P MAS-NMR (MAS = magic angle spinning) sideband intensity pattern, indicating near-to-axial symmetry of the shielding tensor with a maximum shielding component of −60 ppm vs 85% H_3PO_4 parallel to the P=S bond. At P contents exceeding 15 atom %, the MAS-NMR spectra of solid samples give evidence of molecular P_4S_9 and P_4S_{10} groups, whose relative intensity increases with increasing phosphorus content, eventually leading to crystallization at P contents higher than 25 atom %. The distribution of the P atoms over the glass structure is investigated on the basis of homonuclear ^{31}P dipolar second moments, M_{2d}, extracted from ^{31}P spin-echo NMR data. These data are compared with simulations based on a variety of assumed atomic distribution models. While the compositional dependence of M_{2d} is generally compatible with randomly distributed S=$PS_{3/2}$ groups, the detailed quantitative results also support the partial segregation of the more phosphorus-rich structural units (such as P_4S_9, P_4S_{10} above 15 atom % P) evidenced from MAS-NMR. Phosphorus–phosphorus bonds are not detected in significant amounts.

Introduction

The phosphorus–sulfur system has been attractive to investigators for many decades.[1-4] Extensive past investigations have resulted in a complete phase diagram and have confirmed the existence of a large number of compositionally well-defined compounds. Among these, the molecular and crystal structures of α-P_4S_3,[5] β-P_4S_3,[6] α-P_4S_4,[7,8] α-P_4S_5,[9] P_4S_7,[9,10] P_4S_9,[11] and P_4S_{10}[9] are well-known from X-ray crystallography. NMR spectroscopic evidence also suggests the existence of an additional compound P_4S_8[12] and a variety of sulfur-rich species with S/P ratios exceeding the P_4S_{10} stoichiometry.[13] Furthermore, less well-characterized polymorphs have been reported for P_4S_4,[7] P_4S_5,[14] P_4S_{7-x} ($x < 1$),[15] and P_4S_9.[16]

In addition, phosphorus and sulfur are known to form glasses with compositions ranging from 0 to ca. 25 atom % P.[17-19] It has been only recently that glasses of this kind have attracted interest in materials science because of their infrared transmitting properties, which offer new opportunities for optical wave-guide applications.[20] Furthermore, lithium-containing glasses based on phosphorus and silicon sulfide appear promising candidates for solid electrolytes in low equivalent weight batteries.[21]

The structural elucidation of such disordered systems, which may provide useful guidelines for tailoring their physicochemical properties, requires techniques that are not inherently limited by the lack of periodicity. However, most techniques, such as EXAFS, XPS, Moessbauer spectroscopy, neutron diffraction, and IR/Raman spectroscopy, on which structural models in non-oxide chalcogenide glasses have previously been based, suffer from the drawbacks that the interpretation is not straightforward, that quantitative information is difficult to obtain, and that ordered environments tend to be emphasized.

Solid-state NMR techniques avoid such problems while offering new powerful approaches to glass structure. Recently, the increased spectroscopic resolution obtained through the use of fast magic angle spinning has enabled the identification and quantitation of specific short-range-order environments and thus provided extremely valuable information on the structure of many oxide-based systems, specifically silicate[22-25] and phosphate[26] glasses. Such investigations have confirmed that the distribution function of structural parameters in oxidic glasses is not a featureless continuum but that these glasses contain well-defined short-range-order environments ("discrete site hypothesis"), comparable with Zachariasen's description of network modification.[27] While a great deal of knowledge has been accumulated on oxidic glasses to date, the systematic NMR investigation of structural principles in chalcogenide glasses has just begun.[28-32] One of the aims of

(1) Forthmann, A.; Schneider, A. *Z. Phys. Chem. (Munich)* **1966**, *49*, 22.
(2) Moedritzer, M.; Van Wazer, W. R. *J. Inorg. Nucl. Chem.* **1963**, *25*, 683.
(3) Vincent, H.; Vincent-Forat, C. *Bull. Soc. Chim. France* **1973**, 499.
(4) Treadwell, M.; Beeli, Ch. *Helv. Chim. Acta* **1935**, *18*, 1161.
(5) Leung, Y. C.; Wazer, J.; Van Houten, S.; Vos, A.; Wiegers, G. A.; Wiebenga, E. H. *Acta Crystallogr.* **1957**, *10*, 574.
(6) Chattopadhyay, T.; Gmelin, E.; Von Schnering, H. G. *J. Phys. Chem. Solids* **1982**, *43*, 925.
(7) Minshall, P. C.; Sheldrick, G. M. *Acta Crystallogr.* **1978**, *B34*, 1326.
(8) Griffin, A. M.; Minshall, P. C.; Sheldrick, G. M. *J. Chem. Soc., Chem. Commun.* **1976**, 809.
(9) Vos, A.; Othof, R.; Van Bolhuis, F.; Botterweg, R. *Acta Crystallogr.* **1965**, *19*, 864.
(10) Dixon, D. T.; Einstein, F. W. B.; Penfold, B. R. *Acta Crystallogr.* **1965**, *18*, 221.
(11) Hilmer, W. *Acta Crystallogr.* **1969**, *B25*, 1229.
(12) Barieux, J. J.; Demarcq, M. C. *J. Chem. Soc., Chem. Commun.* **1982**, 176.
(13) Demarcq, M. C. *Phosphorus Sulfur* **1987**, *33*, 127.
(14) Blachnik, R.; Hoppe, A. *Z. Anorg. Allg. Chem.* **1979**, *457*, 91.
(15) Rodley, G. A.; Wilkins, C. J. *J. Inorg. Nucl. Chem.* **1960**, *13*, 231.
(16) Meisel, M.; Grunze, H. *Z. Anorg. Allg. Chem.* **1970**, *373*, 265.
(17) Heyder, F.; Linke, D. *Z. Chem.* **1973**, *13*, 480.
(18) Monteil, Y.; Vincent, H. *Z. Anorg. Allg. Chem.* **1977**, *428*, 259.
(19) Blachnik, R.; Hoppe, A. *J. Non-Cryst. Solids* **1979**, *34*, 191.
(20) Taylor, P. C. *Mater. Res. Soc. Bull.* **1987**, 36.
(21) Sahami, S.; Shea, S. W.; Kennedy, J. H. *J. Electrochem. Soc.* **1985**, *132*, 985. Kennedy, J. H.; Sahami, S.; Shea, S. W.; Zhang, Z. *Solid State Ionics* **1986**, *18/19*, 368.
(22) Grimmer, A. R.; Mägi, M.; Hähnert, M.; Stade, H.; Samoson, A.; Wieker, W.; Lippmaa, E. *Phys. Chem. Glasses* **1984**, *25*, 105.
(23) Dupree, R.; Holland, D.; McMillan, P. W.; Pettifer, R. F. *J. Non-Cryst. Solids* **1984**, *68*, 399.
(24) Kirkpatrick, R. J.; Smith, K. A.; Kinsey, R. A.; Oldfield, E. *Am. Mineral.* **1985**, *70*, 106.
(25) Schneider, E.; Stebbins, J. F.; Pines, A. *J. Non-Cryst. Solids* **1987**, *89*, 371.
(26) Villa, M.; Chiodelli, G.; Scagliotti, M. *Solid State Ionics* **1986**, *18/19*, 382.
(27) Taylor, P. C.; Friebele, E. J. J. *Non-Cryst. Solids* **1974**, *16*, 375. Zachariasen, W. W. *J. Am. Ceram. Soc.* **1932**, *54*, 3841.
(28) Eckert, H.; Liang, C. S.; Stucky, G. D. *J. Phys. Chem.* **1989**, *93*, 452.
(29) Eckert, H.; Zhang, Z.; Kennedy, J. H. *J. Non-Cryst. Solids* **1989**, *107*, 271.
(30) Eckert, H.; Zhang, Z.; Kennedy, J. H. *Mater. Res. Soc. Symp. Proc.* **1989**, *135*, 259.

0022-3654/90/2094-2145$02.50/0

the present study is the identification and characterization of the nearest-neighbor environments in chalcogenide glasses, specifically of the phosphorus–sulfur system. To this end, we will use magic angle spinning (MAS) NMR to determine the isotropic and anisotropic chemical shift properties of these glasses and of crystalline model compounds.[28]

Previous investigations by other techniques have also suggested that a typical feature of the structure of non-oxide chalcogenide glasses is the presence of clusters, constituting a substantial degree of intermediate-range order.[33-35] As demonstrated previously by us,[32] NMR techniques are well suited to test such ideas in non-oxidic glasses. The method is based on the measurement of the magnitude and the compositional dependence of the dipole–dipole couplings between the ^{31}P nuclear spins, which depend on the average internuclear distances.[36] Using a selective spin-echo sequence, we have previously measured the strength of such internuclear interactions in P–Se glasses, hence enabling us to test a variety of atomic distribution models.[32] In the present study, we extend this approach to the phosphorus–sulfur system.

Experimental Section

Sample Preparation and Characterization. Yellow-green glasses containing 5–25 mol % phosphorus were prepared, according to literature methods, within evacuated Vycor ampoules, heated at 700 °C for 1–2 days, and quenched by turning off the furnace. Glasses containing more than 20 atom % P were quenched in water. All sample manipulations were carried out in a dry box. Glass transition temperatures were measured on a Du Pont Model 912 dual-sample differential scanning calorimeter (DSC), using heating rates of 5–10 °C/min. The glass transition temperatures of most of the glasses were found in good agreement (within 5–10 °C) with literature values,[17-19] while others (specifically around 15 atom % P) were consistently found 25–30 °C higher than previously reported. To assess the influence of sample preparation temperatures, two samples containing 14.9 atom % P were synthesized at 450 and 750 °C, respectively. Both the T_g values (111 °C, versus a literature value of 85 °C) and the NMR parameters were identical for these samples within the error limits. Glasses with P contents above 20 atom % tend to recrystallize under DSC conditions. Formation of completely amorphous samples was also verified by X-ray powder diffraction, with use of a Scintag diffractometer. The synthesis and characterization of P_4S_3, P_4S_7, P_4S_9, and P_4S_{10}, used here as crystalline reference compounds, has been described elsewhere.[28] α-P_4S_5 was synthesized from P_4S_3 and S_8 in the presence of a trace of I_2.[37] Its identity was confirmed by X-ray powder diffraction. It melts under decomposition above 150 °C, in agreement with literature data.[14] The ^{31}P liquid-state NMR spectrum shows a complex second-order multiplet (ABCX system) as expected (see Figure 3a for the molecular structure). Analysis of this spectrum, using the GEMSIM software, yields the following parameters: δ_A = 92.1 ppm, δ_B = 125.4 ppm, δ_C = 127.2 ppm, and δ_X = 234.0 ppm; J(AB) = 175 Hz, J(AC) = 290 Hz, J(AX) = 53 Hz, J(BC) = 120 Hz, J(BX) = 20 Hz, J(CX) = 28 Hz. Although no firm assignment can be made at this time, the magnitude of the spin–spin coupling constant suggests that multiplet A arises from the P atom involved in two P–P bonds. It is also apparent from the coupling constants that the multiplet at 234.0 ppm has to be assigned to the apical $PS_{3/2}$ group, the only one lacking P–P bonding. β-$P_4S_3I_2$ was synthesized from P_4S_3 and I_2 in CS_2 according to the procedure of Topsom and Wilkins.[38] Orange crystals were obtained upon cooling, whose identity (mp = 118.9 °C (literature value 120.5 °C)) was verified by liquid-state NMR, which shows an A_2MX spectrum with the following parameters (literature data in parentheses:[39] δ_A = 93.7 (93.6) ppm, δ_B = 151.4 (151.3) ppm, δ_X = 196.0 (196.1) ppm; J(AM) = 252 (252) Hz, J(AX) = 57 (56) Hz, J(MX) = 82 (82) Hz. Assignment of resonance A to the two iodine-bearing P atoms, resonance M to the central P atom, and resonance X to the apical $PS_{3/2}$ group is straightforward on the basis of intensity and coupling constant arguments.

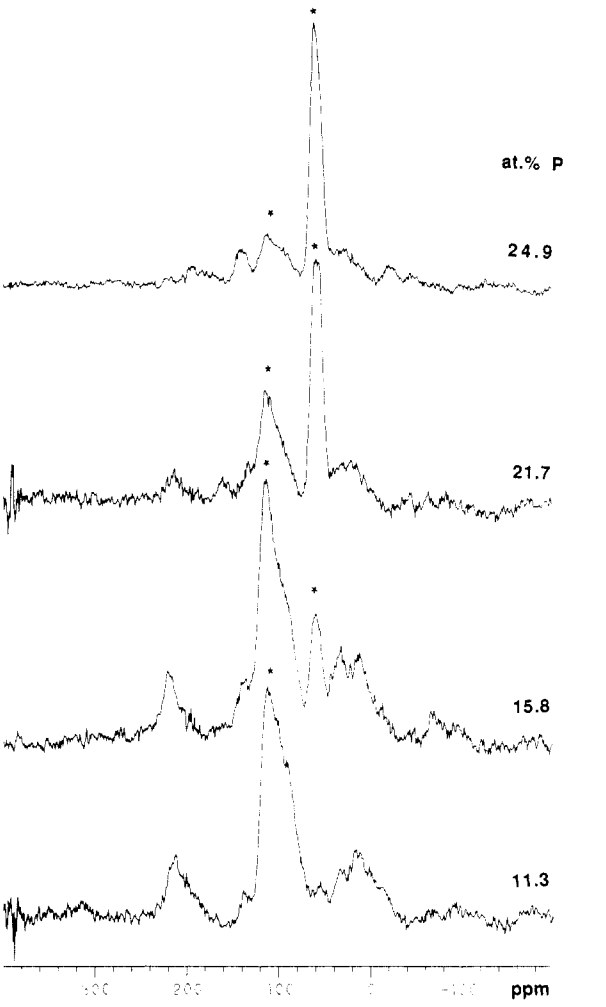

Figure 1. High-speed 121.46-MHz ^{31}P MAS-NMR spectra of P–S glasses as a function of composition. Central lines are indicated by asterisks.

Solid-State NMR Studies. Room-temperature MAS-NMR spectra were obtained at 121.65 and 121.46 MHz on General Electric Model GN-300 and Nicolet Model NT-300 spectrometers, respectively, at variable spinning speeds (5.0–14.0 kHz) using a standard 7-mm as well as a 5-mm ultrahigh-speed MAS-NMR probe (both from DOTY Scientific; spinning speeds ca. 5 kHz and 10–12.5 kHz, respectively). Single-pulse acquisition was used, with 90° pulse lengths of 7.0 and 4.5 μs, respectively. Additional studies were carried out at 202.49 MHz (11.7 T), using a Bruker Model AM-500 spectrometer and a Doty probe. Spectra were typically recorded with 45° pulses with recycle delays of 1–10 min. Experiments using longer recycle delays were shown to leave relative peak area ratios unchanged. All chemical shifts are referenced with respect to 85% H_3PO_4 (downfield shifts positive). Where possible, chemical shift tensor components were deduced from spinning sideband patterns, by the method of Herzfeld and

(31) Lathrop, D. A.; Eckert, H. *J. Non-Cryst. Solids* **1988**, *106*, 417.
(32) Lathrop, D. A.; Eckert, H. *J. Am. Chem. Soc.* **1989**, *111*, 3536.
(33) Price, D. L.; Misawa, M.; Susman, S.; Morrison, T. I.; Shenoy, G. K.; Grimsditch, M. *J. Non-Cryst. Solids* **1984**, *66*, 443. Arai, M.; Johnson, R. W.; Price, D. L.; Susman, S.; Gay, M.; Enderby, J. E. *J. Non-Cryst. Solids* **1986**, *83*, 80.
(34) Phillips, J. C. *J. Non-Cryst. Solids* **1981**, *43*, 37; Phillips, J. C., *J. Non-Cryst. Solids* **1979**, *34*, 153.
(35) Tenhover, M.; Henderson, R. S.; Lukco, D.; Hazle, M. A.; Grasselli, R. K. *Solid State Commun.* **1984**, *51*, 455. Tenhover, M.; Hazle, M. A.; Grasselli, R. K. *Phys. Rev. Lett.* **1983**, *51*, 404. Griffiths, J. E.; Malyj, M.; Espinosa, G. P.; Remeika, J. P. *Phys. Rev. B* **1984**, *30*, 6978.
(36) Van Vleck, J. H. *Phys. Rev.* **1948**, *74*, 1168.
(37) Boulouch, R. *C. R. Hebd. Seances Acad. Sci.* **1904**, *138*, 363.
(38) Topsom, R. D.; Wilkins, C. J. *J. Inorg. Nucl. Chem.* **1956**, *3*, 187.
(39) Blachnik, R.; Kurz, G.; Wickel, U. *Z. Naturforsch., Teil B* **1984**, *39*, 778.

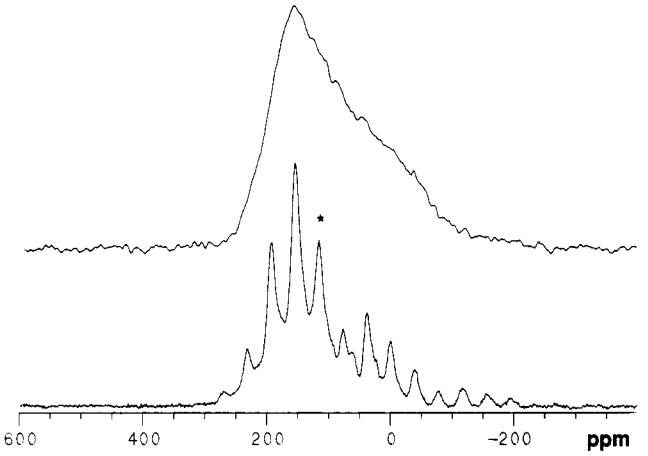

Figure 2. Low-speed 121.65-MHz and wide-line (spin-echo FT) ^{31}P NMR spectra of a P–S glass containing 14.9 atom % phosphorus. The MAS centerband is indicated by an asterisk.

Berger.[40] These values are reported relative to 85% H_3PO_4, with $\sigma_\parallel$ as the most upfield component. All spin-echo NMR studies were carried out at 121.65 MHz under conditions of minimized resonance offsets and spin equilibrium; this necessitated recycle delays of up to 60 min.

Results, Data Analysis, and Assignments

MAS-NMR Characterization of Specific Local Environments in P–S Glasses and Crystalline Model Compounds. Figure 1 shows representative high-speed MAS-NMR spectra obtained on the glasses, indicating systematic changes as a function of composition. At low phosphorus contents, the spectra are dominated by a resonance centered at 112 ± 2 ppm vs H_3PO_4 whereas above 15 atom % P additional sharper resonances at 51 ± 1 and 57 ± 1 ppm become increasingly intense and dominate the spectrum at 25 atom % P. The location of this second resonance is close to those found in solid P_4S_{10} and P_4S_9. Furthermore, when the glasses are treated with CS_2, both the 51 and the 57 ppm peaks diminish, and the liquid-state ^{31}P NMR spectra of the CS_2 extracts show a strong singlet due to P_4S_{10}, the characteristic AB_3 pattern typical[41] of P_4S_9, and the two very weak resonances[42] due to P_4S_7. This experiment indicates the presence of such molecular species in the glass structure. The joint occurrence of P_4S_9 and P_4S_{10} molecules in the glasses is a manifestation of the redox dissociation equilibrium of melted P_4S_{10} previously investigated by Demarq.[43]

Finally, the assignment for the 112 ppm resonance needs to be discussed. Figure 2 shows wide-line and low-speed MAS-NMR data on a glass containing 15 atom % phosphorus, which can be considered representative of glasses with this site.

Since the spin-echo NMR experiments to be discussed below indicate that within the region of glass formation no P–P bonds occur, the task of identifying microenvironments is reduced to that of an unambiguous distinction between $PS_{3/2}$ and $S{=}PS_{3/2}$ groups. Previous detailed studies of chemical shift tensors in a variety of crystalline phosphorus sulfides have shown that the isotropic chemical shifts for both groups are very sensitive to local distortions, resulting in wide chemical shift ranges that show considerable overlap.[28] Therefore, isotropic chemical shifts are unsuitable for discriminating between $PS_{3/2}$ and $S{=}PS_{3/2}$ connectivities. It was shown empirically, however, that, in spite of the considerable variations in δ_{iso}, the anisotropic shielding properties might be more informative for discriminating between these environments. To examine this possibility, additional model compounds containing the $PS_{3/2}$ unit were investigated, specifically P_4S_5 and β-$P_4S_3I_2$. The MAS-NMR spectra are shown in Figure 3. For P_4S_5 we can distinguish four different spinning sideband

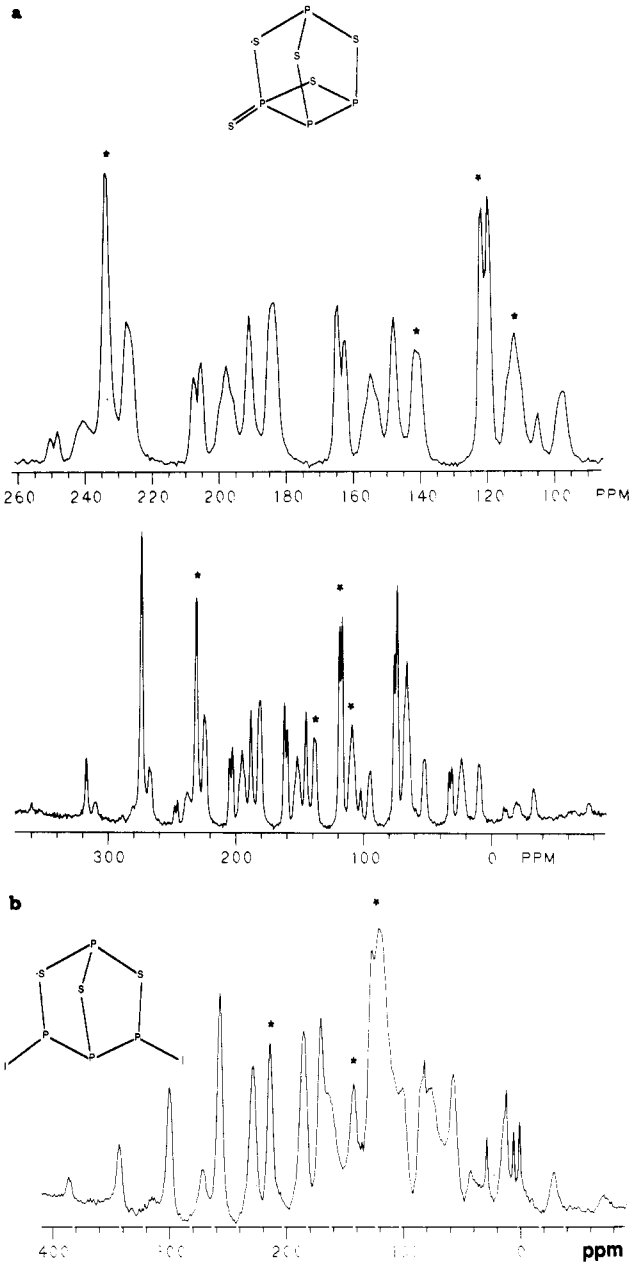

Figure 3. (a) ^{31}P MAS-NMR spectrum at 121.65 MHz of P_4S_5. Top: an expansion of the centerband region. Spinning speed 5.2 kHz. Central lines are indicated by asterisks. (b) ^{31}P MAS-NMR spectrum of β-$P_4S_3I_2$. Central lines are indicated by asterisks. Spinning speed 5.2 kHz.

patterns, in concordance with the four chemically inequivalent P atoms of the molecule. Several of these patterns show indications of peak multiplicity. Comparison with an 11.7-T spectrum reveals that this multiplicity arises from scalar spin–spin coupling. The pattern with the most downfield centerband is assigned to the $PS_{3/2}$ unit, i.e, the only P atom in this molecule that is not involved in P–P bonding. This assignment is based on the liquid-state NMR spectrum discussed above as well as the fact that this particular resonance is the only one lacking any fine structure due to one-bond ^{31}P–^{31}P spin–spin coupling. The assignment differs from the tentative one made by us in a previous publication.[28] The solid-state MAS-NMR spectrum of β-$P_4S_3I_2$ shows three well-resolved MAS-NMR sideband patterns. Tentative assignments, based on the liquid-state NMR data,[39] are included in Table I. One-bond ^{31}P–^{31}P spin–spin couplings cannot be resolved in this case, because the MAS-NMR peaks are substantially broadened by the dipolar interaction of the ^{31}P spins with the quadrupolar ^{127}I nuclei. Table I and Figure 4 give a schematic summary of all of the known chemical shift tensor components for compounds containing either $S{=}PS_{3/2}$ or $PS_{3/2}$ units. It is seen that tetra-

(40) Herzfeld, J.; Berger, A. E. *J. Chem. Phys.* **1980**, *73*, 6021.
(41) Thamm, R.; Heckmann, G.; Fluck, E. *Phosphorus Sulfur* **1982**, *12*, 319.
(42) Brevard, C.; Demarq, M. C. *Chem. Phys. Lett.* **1981**, *82*, 167.
(43) Demarq, M. C. *Phosphorus Sulfur* **1981**, *11*, 65.

TABLE I: Solid-State NMR Chemical Shifts and Principal Tensor Components for $PS_{3/2}$ and $S{=}PS_{3/2}$ Groupings in Crystalline Phosphorus Sulfides

grouping	δ_{iso},[a] ppm	δ_{11},[b] ppm	δ_{22},[b] ppm	δ_{33},[b] ppm
$PS_{3/2}$				
P_4S_9	57.7	1	57	113
P_4S_5	233.7[c]	102	290	309
P_4S_3	91.0	7	30	236
	84.5	0	14	240
β-$P_4S_3I_2$	214.0[d]	40 ± 20[e]	220 ± 20[e]	380 ± 20[e]
$S{=}PS_{3/2}$				
P_4S_{10}	51.6	−57	106	106
	49.7	−55	94	110
P_4S_9	67.8	−40	104	139
	64.0	not determined (peak overlap)		
	61.6	not determined (peak overlap)		
P_4S_7	111.9	−49	137	248
	112.8	−44	115	267
glass				
(5–15%)	112 ± 2	−55 ± 20	190 ± 20	190 ± 20

[a] ±0.1 ppm vs external 85% H_3PO_4, unless noted otherwise. [b] ±5 ppm vs external 85% H_3PO_4, unless noted otherwise. [c] Additional resonances in the solid-state spectra are centered at 140.5, 120.4, and 111.7 ppm. [d] Additional resonances in the solid-state spectra are centered at 142.3 and 120.9 ppm. [e] Low precision due to strong peak overlap.

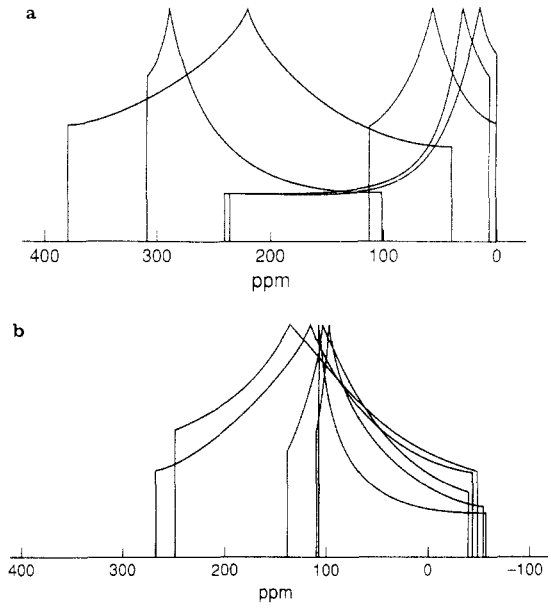

Figure 4. (a) Schematic drawings of the chemical shift anisotropy powder patterns for $PS_{3/2}$ groups occurring in the various phosphorus–sulfur compounds of Table I. (b) Schematic drawings of the chemical shift anisotropy powder patterns for $S{=}PS_{3/2}$ groups occurring in the various phosphorus–sulfur compounds of Table I.

hedral $S{=}PS_{3/2}$ groups can be identified by a unique value of the most shielded component δ_{11} in the vicinity of −55 ppm. The line shape reveals further that the shielding along the C_{3v} axis (which corresponds to the chemical shift tensor unique axis) is the greatest. In contrast, the magnitudes, orientations, and isotropic and anisotropic chemical shift components are found highly variable for $PS_{3/2}$ groups, hence making it impossible to identify such units by a characteristic NMR signature. We point out, however, that none of the $PS_{3/2}$ model compounds studied show any anisotropic shift component as far upfield as −55 ppm, the value observed for the 112 ppm resonance in the glasses. This, in connection with the fact that the latter value coincides with that determined for all known δ_{11} components of $S{=}PS_{3/2}$ groups, strongly suggests a corresponding assignment to such a unit.

Atomic Distribution of P Atoms in the Glass Structure As Determined by Homonuclear Dipole–Dipole Coupling Strengths. As previously demonstrated for the phosphorus–selenium system, measurements of internuclear dipole–dipole coupling strengths

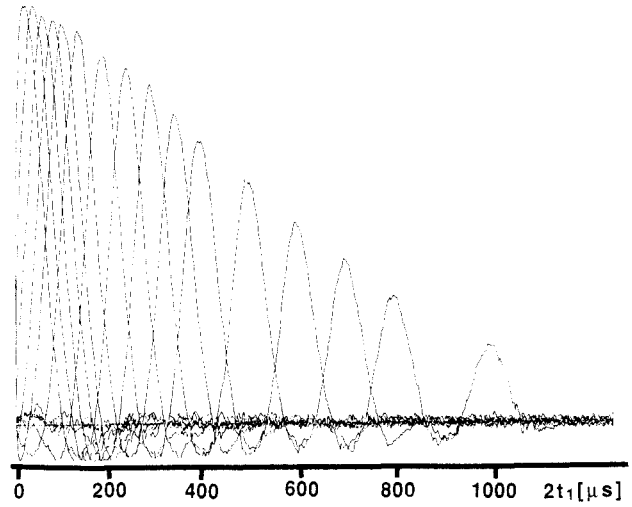

Figure 5. Collection of ^{31}P spin echoes for a P–S glass containing 14.9 atom % phosphorus.

afford a straightforward way of investigating proposed atomic distribution models in non-oxide chalcogenide glasses.[32] The dipolar coupling in magnetically less dilute systems (such as the ones under study here), is usually expressed in terms of a statistical quantity, the second moment M_{2d} of the resonance line. Assuming the dominance of homonuclear dipole–dipole couplings over other types of anisotropic perturbations in the solid state, M_{2d} can be calculated from the internuclear distances d_{ij} by the van Vleck theory,[36] which in the case of a polycrystalline material predicts

$$M_{2d} = {}^3/_5(\mu_0/4\pi)^2 I(I+1)\gamma^4\hbar^2 N^{-1}\sum d_{ij}^{-6} \qquad (1a)$$

or

$$M_{2d} = {}^4/_{15}(\mu_0/4\pi)^2 I(I+1)\gamma^4\hbar^2 N^{-1}\sum d_{ij}^{-6} \qquad (1b)$$

where γ is the gyromagnetic ratio of the nucleus under consideration, I is the spin quantum number, and N is the number or nuclei involved. Equation 1a is appropriate, if the line shape is dominated by homogeneous broadening (due to homonuclear dipole–dipole coupling). Equation 1b has to be used, however, if inhomogeneous sources of line broadening (chemical shift anisotropy or chemical shift distribution) predominate, since the resulting spectral dispersion suppresses the quantum mechanical ("flip–flop") term in the truncated dipolar Hamiltonian.[44] In particular, the pulse sequence 90°–t_1–180° refocuses all interactions linear in I_z (i.e., heterodipolar ^{31}P–^{33}S couplings, chemical shift anisotropies, and chemical shift distribution), resulting in formation of an echo at time $2t_1$. The height of this echo decreases with increasing t_1, because homonuclear ^{31}P–^{31}P spin–spin interactions are not refocused. In the case of multiple spin interactions, the decay of the echo height $I(2t_1)$ as a function of $2t_1$ can often be approximated as a Gaussian:[45,46]

$$I(2t_1)/I(0) = \exp[-[M_{2d}(2t_1)^2/2]]$$

Thus, the homonuclear dipolar second moment M_{2d} can be determined by spin-echo experiments with systematic incrementation of the evolution time $2t_1$. To obtain well-defined spin echoes, it is crucial that the strength of the interactions linear in I_z be at least comparable in magnitude to the ^{31}P–^{31}P dipolar coupling strength to be measured. Figure 5 shows a typical collection of spin echos as a function of evolution time $2t_1$ for a selected composition. The corresponding semilogarithmic plot ($-\ln\{I(2t_1)/I(0)\}$ against $(2t_1)^2$) (Figure 6) shows that the decay is Gaussian in character over a wide range of $2t_1$ ($2t_1 \leq 400$ μs). Linear regression fits have been obtained for all samples within the time

(44) Abragam, A. *The Principles of Nuclear Magnetism*; Clarendon Press: Oxford, 1964.
(45) Engelsberg, M.; Norberg, R. E. *Phys. Rev.* **1972**, *B5*, 3395.
(46) Fenzke, D.; Freude, D.; Müller, D.; Schmiedel, H. *Phys. Status Solidi* **1972**, *50b*, 209.

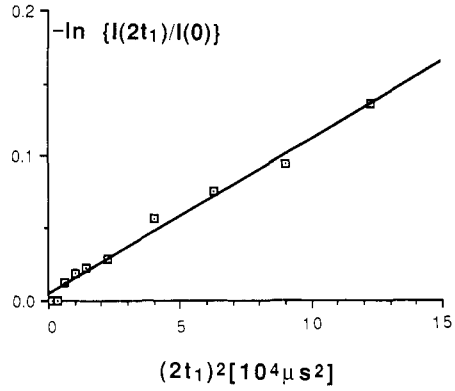

Figure 6. Plot of $-\ln \{I(2t_1)/I(0)\}$ as a function of evolution time $(2t_1)^2$ in the NMR spin-echo series $90°-t_1-180°-t_1$–acquire, for a P–S glass containing 14.9 atom % phosphorus.

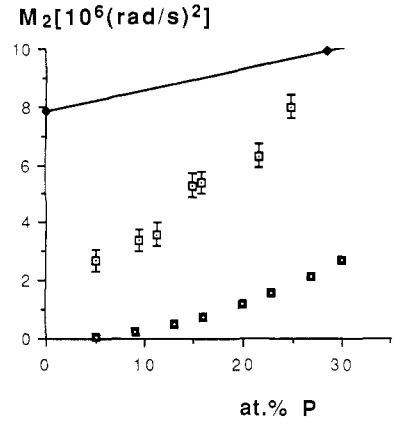

Figure 7. Experimental dipolar ^{31}P second moments, M_{2d} (open squares), and comparison with two simplistic models, involving uniform distribution (filled squares) and P_4S_{10} clusters (upper line). The least-squares-fit line through the points characterizing the cluster model is given by M_{2d} [10^6 (rad/s)^2] = 7.865 + (0.072 atom % P); R = 1.00.

interval $0 \le 2t_1 \le 400$ μs. The time-domain measurement yields M_{2d} in units of rad^2/s^2, i.e., $4\pi^2$ times the value obtained from the numerical analysis of a dipolarly broadened line shape in the frequency domain. We have shown previously that the application of this technique to crystalline phosphorus sulfides and selenides leads to experimental M_{2d} values close to the ones calculated from the crystal structures, hence confirming the experimental reliability of this approach.[32] Other applications of this technique to derive atomic distribution models in glasses have been described in the literature.[47-49]

The compositional dependence of the M_{2d} values obtained for the glasses is shown in Figure 7, where they are contrasted with two simplistic atomic distribution models. A uniform distribution model in which P–P distances are maximized was simulated by arranging the number of P atoms per cm^3 (calculated from the P and S contents and the experimental densities[17]) in a cubic lattice. A distribution based on P_4S_{10} clusters was simulated by interpolation between the experimental M_2 value determined for crystalline P_4S_{10} (28.6% P) and the calculated intramolecular contribution (80%) of this value (near 0% P). Figure 7 clearly shows that both distribution models can be ruled out on the basis of our experiments. Alternatively, we have tested a random distribution model. Figure 8 shows a comparison of the data with a calculation based on a tailored random distribution of P atoms over a cubic zincblende lattice. The zinc blende model modified in this fashion affords quite a realistic description, because the two principal types of bonding, P–S and S–S, are characterized

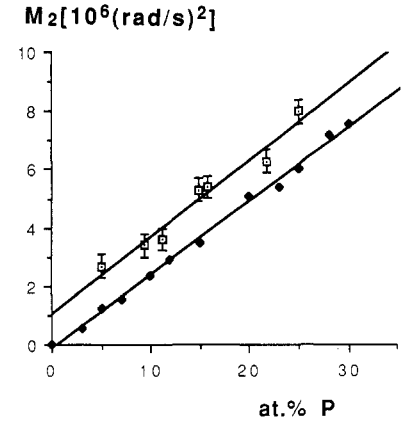

Figure 8. Experimental dipolar ^{31}P second moments, M_{2d} (open squares), and comparison with the values calculated from a tetrahedral zinc blende lattice, using a tailored random distribution model excluding P–P bonds (filled symbols). The least-squares-fit line through the points characterizing the random distribution model is given by M_{2d} [10^6 (rad/s)^2] = −0.131 + (0.253 atom % P); R = 1.00. The least-squares-fit line through the experimental points is given by M_{2d} [10^6 (rad/s)^2] = 1.069 + (0.264 atom % P); R = 0.98.

by essentially identical interatomic distances. The lattice constant was taken to be 4.735 Å, corresponding to a nearest-neighbor distance of 2.05 Å. This value reflects the average P–S distance in P_4S_{10}.[9] (For simplicity, no differentiation was made between P—S single and P=S double bonds.) The number of the P atoms per unit volume was determined from the composition (atom percent P) of the glass in question and the experimental densities. Perfect chemical ordering, i.e., the complete absence of P–P bonds, was assumed. The second moment was calculated from the van Vleck formula for the P atoms in the central 15 Å × 15 Å × 15 Å volume, with use of the generated interatomic distances to all P atoms in the total volume of 45 Å × 45 Å × 45 Å. This includes all P–P distances below 15 Å. The lattice sum was shown to converge well at larger volumes of the total lattice. Calculated M_2 values for larger lattices were less than 1% higher than for the above calculation. Typically, the average over n lattice sums over $1500/n$ atoms was taken, n being on the order of 50, depending on P content.

We note that an expression for M_2 applying to the case of a random distribution over a cubic lattice has been given in the literature.[50] Rather than using this expression, we choose here to carry out a lattice calculation, in order to be able to tailor our calculation such that we can explicitly exclude P–P bonding. Furthermore, it has been pointed out that for a random distribution, in the limit of high dilution the second moment is of minor importance as a measure of the line width because the dipolar line shape becomes more Lorentzian in nature.[50] This is not observed here, partly because the P concentrations are still moderately high (5% or more) and partly because the P distribution is not truly random (no P–P bonds are present).

Discussion and Conclusions

Figures 7 and 8 indicate the utility of dipolar NMR in differentiating quantitatively between various atomic distribution models in glasses. The experimental second moment data are generally well compatible with the above statistical model (Figure 8), especially when the compositional dependencies of M_{2d} (i.e., the slopes in Figure 8) are considered. However, for all compositions, the experimental second moments are systematically larger than calculated, indicating that some degree of segregation may occur here. This segregation effect is apparent in the MAS-NMR data and in the liquid-state spectra of the CS_2 extracts, both of which clearly reveal the presence of some P_4S_{10} and P_4S_9 in glasses with substoichiometric phosphorus contents (15.8 atom % P and above). Although these molecules are not

(47) Reimer, J. A.; Duncan, T. M. *Phys. Rev. B* **1983**, *27*, 4895.
(48) Duncan, T. M.; Douglass, D. C.; Csencsits, R.; Walker, K. L. *J. Appl. Phys.* **1986**, *60*, 130.
(49) Douglass, C. C.; Duncan, T. M.; Walker, K. L.; Csencsits, R. *J. Appl. Phys.* **1985**, *58*, 197.

(50) Abragam, A. *Principles of Nuclear Magnetism*; Clarendon Press: Oxford, 1983; p 125 (paperback issue).

present in glasses with less than 15 atom % phosphorus, the data in Figure 8 suggest that partial phosphorus segregation persists even at lower P contents. This may be understood in terms of a larger-than-statistical probability of P-S-P linkages. Furthermore, the spin-echo NMR data confirm that P-P bonds are essentially absent in P-S glasses.

In summary, the present study illustrates that modern solid-state NMR techniques can provide valuable information concerning the chemical segregation processes and the structural units present in non-oxide chalcogenide glasses. It is instructive to compare the present results on the P-S system with those recently obtained on the homologous system phosphorus-selenium.[32] Both systems have in common that P-P bonds are absent in the compositional region considered (0-25 atom % P); however, the fraction of tetrahedral groups is markedly reduced in the P-Se system, reflecting a more efficient competition of homoatomic (Se-Se) with heteroatomic (P=Se) bond formation. In agreement with this finding, molecular clusters analogous to P_4S_9 and P_4S_{10} are absent in the system phosphorus-selenium. On the other hand, MAS-NMR data indicate that P-Se glasses with 50 atom % P or more contain significant amounts of molecular P_4Se_3 units.[51] It seems, therefore, that molecular clusters are a common characteristic feature in phosphorus chalcogenide glasses. However, the NMR studies show, that these molecules, which have stoichiometries corresponding to the stable bordering crystalline phases, only occur in the vicinity of the glass-forming boundaries.

Acknowledgment. We are grateful for financial support by the UCSB Academic Senate. Acknowledgment is made to the donors of the Petroleum Research Fund, administered by the American Chemical Society, for financial support of this research. Partial funding was also provided by a grant from the U.S. Department of Energy (Contract No. DE AS03-76SF00034) to Professor R. G. Pearson (UCSB). We are indebted to Professor Pearson for his support. We also thank Cheryl Liang for a sample of P_4S_5.

Registry No. P, 7723-14-0; S, 7704-34-9.

(51) Lathrop, D.; Eckert, H. *J. Phys. Chem.* **1989**, in press.

Anion Dependence of the Complexation of Na^+ with the Macrocycle 18C6 in Propylene Carbonate

Licesio Rodriguez,[†] Edward M. Eyring,[‡] and Sergio Petrucci*,[†]

Weber Research Institute, Long Island Center, Polytechnic University, Farmingdale, New York 11735, and Department of Chemistry, University of Utah, Salt Lake City, Utah 84112 *(Received: March 7, 1989; In Final Form: July 13, 1989)*

Ultrasonic relaxation spectra in the frequency range ~1-500 MHz for $NaB\Phi_4$ ($\Phi = C_6H_5$), $NaClO_4$, and NaSCN in the concentration range 0.1-0.5 M and in the solvent propylene carbonate (PC) at 25 °C are reported. This solvent has been selected because, despite its high dielectric permittivity, its donor number is relatively low. Thus in the competition for sites in the first coordination sphere of metal cations, macrocycles and anions will be favored over solvent molecules. Previous kinetic studies of decomplexation of electrolytes in PC and other solvents of low donor numbers (such as acetonitrile and nitromethane) by NMR techniques have indicated a bimolecular mechanism involving excess cation: $MC^+ + {}^*M^+ \rightleftarrows {}^*MC^+ + M^+$, where M^+ denotes a metal cation and C denotes a macrocycle. The present work shows a dependence of the amplitude of the ultrasonic absorption spectra on the nature of the electrolyte (anion) for the same cation. This raises the question of whether the bimolecular mechanism is simply a reflection of anion vs macrocycle competition for the first-coordination sphere of the cation, namely $MC^+ + X^- \rightleftarrows MX + C$, where X^- denotes the anion. Indeed in solvents of much lower permittivity such as ethers, the attack of the crown ether C on the substrate, consisting of an ion pair MX (according to the reverse of the above scheme) has already been established. The present study provides experimental evidence that the bimolecular mechanism of metal-ion complexation by macrocycles touted by NMR spectroscopists could have its origins in the availability of a high concentration of anions.

Introduction

Investigations of the rates of complexation of alkali-metal cation by crown ether macrocycles with an ultrasonic relaxation technique[1] have established the general application of the Eigen-Winkler mechanism of stepwise solvent substitution[2]

$$MS^+ + C \underset{k_{-0}}{\overset{k_0}{\rightleftarrows}} M^+SC \underset{k_{-1}}{\overset{k_1}{\rightleftarrows}} MC^+ \underset{k_{-2}}{\overset{k_2}{\rightleftarrows}} (MC)^+ \qquad (1)$$

where MS^+ is the solvated cation, C the macrocycle, M^+SC a solvent-separated species, MC^+ the contact or exclusive species, and $(MC)^+$ the inclusive species with the metal imbedded in the cavity of the ligand. If the overall complexation (formation) constant K_Σ is high in scheme 1, at the concentrations attainable by ultrasonic techniques, the above reaction scheme reduces, for all practical purposes, to[1]

$$M^+SC \underset{k_{-1}}{\overset{k_1}{\rightleftarrows}} MC^+ \underset{k_{-2}}{\overset{k_2}{\rightleftarrows}} (MC)^+ \qquad (2)$$

In solvents of very low permittivity such as ethers, the electrolyte is heavily associated to form ion pairs MX and at times to dimers or quadrupoles $(MX)_2$. The overall reaction scheme then becomes[3]

$$(MX)_2 \rightleftarrows 2MX$$

$$MX + C \rightleftarrows MC^+ + X^- \qquad (3)$$

where the first equilibrium establishes a competition for MX (either to dimerize or to be attacked by C).

In aprotic solvents of intermediate permittivity but low donor number such as propylene carbonate ($\epsilon_{25} = 64.4$; DN = 15.1), acetonitrile ($\epsilon_{25} = 35.95$; DN = 14.1), and nitromethane ($\epsilon_{25} = 35.94$; DN = 2.7), recent work by NMR techniques[4] has found

[†] Polytechnic University.
[‡] University of Utah.

(1) Chen, C.; Wallace, W.; Eyring, E. M.; Petrucci, S. *J. Phys. Chem.* **1984**, *88*, 2541; **1985**, *89*, 1357. Wallace, W.; Eyring, E. M.; Petrucci, S. *J. Phys. Chem.* **1984**, *88*, 6353.
(2) Eigen, M.; Winkler, R. M. In *Neurosciences: Second Study Program*; Schmidt, F. O., Ed.; Rockefeller University Press: New York, 1970; p 685.
(3) Farber, H.; Petrucci, S. *J. Phys. Chem.* **1981**, *85*, 1396. Richman, H.; Harada, Y.; Eyring, E. M.; Petrucci, S. *J. Phys. Chem.* **1985**, *89*, 2373.

0022-3654/90/2094-2150$02.50/0